Proceedings World Geothermal Congress 2020+1
Reykjavik, Iceland, April - October 2021

The Study of Optimal Geothermal Well Capacity Evaluation on an Innovative Similar Capacity Test Model

David T.W. Lin, Chun Ping Jen, Yi Chun Du, Jui Ching Hsieh and Bo Heng LEE

Inst. Mechatronic System Eng., National Univ. of Tainan, Tainan, Taiwan

david@mail.nutn.edu.tw

Keywords: Geothermal well, Capacity test, Thermal resistance, Brinkman model, Optimization

ABSTRACT

Nowadays, there is no effective method to evaluate the potential of geothermal well but capacity test. This is due to the poor-known thermal-fluid information about the reservoir. The purpose of this research is to propose a Similar Capacity Test Model (SCTM) for evaluating the capacity of the geothermal well. This proposed similar capacity test model consists of the Brinkman model conjugated with heat transfer model simulated as the reservoir and the pipe flow model as the well. First, the validation of this similar capacity test model of single well IC 13 in Chingshui, Taiwan will be build based on the geometry, well temperature, mass flow rate in in-situ. Then, the thermal resistance of IC 13 can be obtained. The capacity will be optimized by this proposed model combined with the simplified conjugated gradient method for obtaining the best flow rate to find the optimal heat extraction. In the thermal resistance view, the key technology will be proposed for building the reliable evaluated model of geothermal power generation.

1. INTRODUCTION

Geothermal energy includes reservoir, well and power plant. The important issues are heat and mass transfer, chemical reaction, geoscience and the system of power plant. The porous heat transfer in the reservoir, the two phase flow in the well, the minization, and many complicated problem will be solved in the field of geothermal energy.

Lots of researches investigation the geothermal issues. Only in the heat extraction part, the long-term investigation of in-situ (ex. Cladouhos, 2016), the simulated model (ex. Verma and Preuss, 1986) is proposed prosperously. Gallup (2009) reviews many geothermal technology and the discussions of EGS. Jiang et al. (2014) propose a three dimensional transient model based on the two energy balance equations to obtain the heat transfer of the interaction between fluid and rock. The THM model is proposed by the Cao et al. (2016). The stress can be evaluated form the change of temperature and pressure. Shook and Suzuki (2017) use the tracers and temperature to estimate fracture surface area of EGS reservoirs to obtain the heat transfer. The design of multiwell is investigated by Chen et al. (2015). The uniform porous medium is assumed. They obtain the reasonable location of injection well will enhance the heat extraction. The commercial package of COMSOL is used to simulate the effects of isothermal of non-isothermal fluids on the reservoir by Kim et al. (2015).

The simulated model validated based on the in-situ information is an important issue. Sun et al. (2017) evaluates the heat extraction in EGS with thermal-hydraulic-mechanical coupling method based on discrete fractures model. The geothermal system in Habanero, Austria is investigated for validating this model. Jacquey et al. (2016) simulate the Groß Schönebeck reservoir by THM model and discuss the duration and thermal breakthrough time based on the porosity and permeability. Llanos et al. (2015) simulate the heat extraction of the Habanero EGS, the velocity in the four kinds of well location are compared. Jeanne et al. (2014) build a EGS model of Northwest Geysers，and derived in the evolution and profile of micro seismic during injected water times about 10 months.

Biagi et al. (2015) use TOUGH to simulate the EGS and process the optimization by genetic algorithm. The best operated conditions are obtained based on the cooling of reservoir derived from the duration. Our team (Lin et al., 2019) propose the self-developed optimal method to find the best heat extraction of CO_2-EGS.

Lots of parameters should be noticed and many problems and interactions have to clarify their roles in the geothermal problems. Therefore, this study proposes a simplify model to handle the heat extraction. The key feature will be treated from a thermal resistance view. This study introduces the process of this method and a case study – the well of IC13, Chingshui, Taiwan to present the excellent results of this method.

2. METHOLODGY

A similar capacity model is proposed firstly. The thermal resistance of the well is represented the characteristics of the well. The temperature profile of the well can be obtained from the capacity test of in-situ and the single well model. The thermal resistance of this well can be calculated from the heat dissipation and temperature difference between well and environment. This similar capacity test model consists of the Brinkman model conjugated with porous heat transfer model simulated as the reservoir and the pipe flow model as the well. The thermal dispersivity of this numerical model will be obtain from the fitting of the experimental results. In addition, the optimization of this model will process to obtain the optimal operated condition. The schematic diagram and process of similar capacity test model is shown in Fig.1&2.

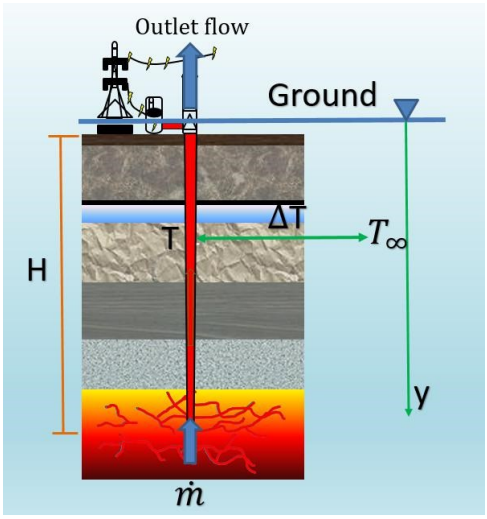


Fig. 1. The schematic diagram of similar capacity test model.

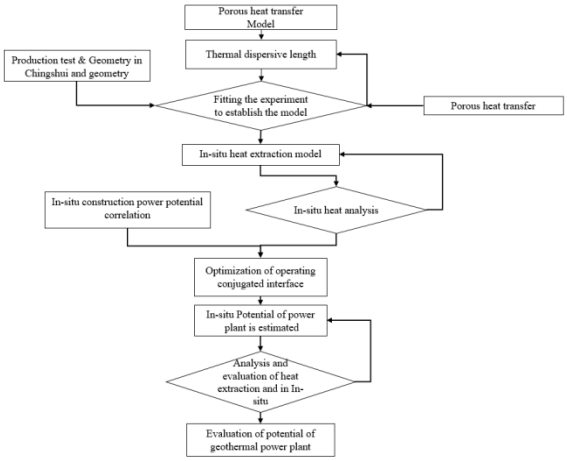


Fig. 2. The process of similar capacity test model.

2.1 Single Well Model

In this study, a 3D porous Brinkman model combined with heat transfer model is established by finite element method(COMSOL, 2014) and based the geometry, boundary of the experimental test section. The simulated model is assumed as the part of reservoir of geothermal well. The schematic diagram of this model is shown in Fig.3. The heat and mass transfer analysis are built by this model.

The governing equations of non-porous medium are described as below:

Continuity equation is:

$$\frac{\partial \rho}{\partial t} + \nabla \cdot (\rho u) = 0 \tag{1}$$

Momentum equation is:

$$\rho \frac{\partial u}{\partial t} + \rho(u \cdot \nabla)u = \nabla \cdot \left[-pI + \mu(\nabla u + (\nabla u)^T) - \frac{2}{3}\mu(\nabla \cdot u)I\right] + F \tag{2}$$

where μ is viscosity; u is velocity; ρ is fluid density; p is pressure and F is forced term.

The governing equations of the Brinkman model are described as below:

Continuity equation is:

$$\frac{\partial}{\partial t}(\varepsilon \rho) + \nabla \cdot (\rho u) = Q_{br} \tag{3}$$

Momentum equation is:

$$\frac{\rho}{\varepsilon}\left(\frac{\partial u}{\partial t}+(u\cdot\nabla)\frac{u}{\varepsilon}\right)$$
$$=-\nabla p+\nabla\cdot\left[\frac{1}{\varepsilon}\left\{\mu\left(\nabla u+(\nabla u^{T})\right)-\frac{2}{3}\mu(\nabla\cdot u)I\right\}\right]-\left(\frac{\mu}{\kappa}+\frac{Q_{br}}{\varepsilon^{2}}\right)u+F \quad (4)$$

where ε is porosity; κ is permeability and Q_{br} is mass force.

The Fourier's law of porous medium is described as below:

$$\frac{\partial}{\partial t}\left[(1-\varepsilon)\rho_{p}C_{p,p}T_{p}\right]-(1-\varepsilon)\nabla\cdot\left(k_{p}\nabla T_{p}\right)=0 \quad (5)$$

Energy balance equation is:

$$\frac{\partial}{\partial t}\left[\varepsilon\rho_{f}C_{p,f}T_{f}\right]+\nabla\cdot\left(\rho_{f}C_{p,f}DT_{f}\right)-\varepsilon\nabla\cdot\left(k_{f}\nabla T_{f}\right)=0 \quad (6)$$

where T is temperature; C_p is specific heat; k is thermal conductivity, D is Darcy flow and the subscript label f means fluid and p is media.

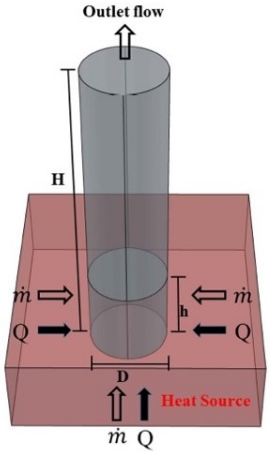


Fig.3 The schematic diagram of single well model.

2.1 Thermal Dispersion

Comparing the realistic kilometer scale of reservoir and meter-scale porous experiment, the random fracture in the reservoir can be assumed as the pipe flow or uniform porous flow. A high pressure porous heat transfer experiment proposed as the reservoir is reasonable in this study. The schematic diagram of the experimental system is shown in Fig. 4. The experimental system consists of a high pressure pump, preheated water bath, cooling water bath, heating unit, test section of reservoir, differential pressure gage, flow meter, and data logger. The photograph of the experimental system is shown in Fig. 5. Here, water is pumped into the preheated water bath at various pressure (7.5, 9, 10, 11 and 12.5MPa) and heated over 40℃ . The inside, outside diameter and length of test section are 29.9, 55.0, and 235.0 mm. The porous media is silica-base particles. For comparing the effects of porosity, the empty of test section is also examined. The porosity is approximately 0.2 and 0.39 based on the mean mass diameter of particle is 1.54 and 2.03 mm, respectively.

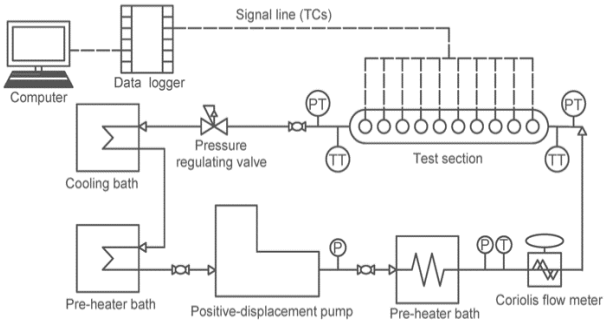


Fig. 4. The schematic diagram of experimental system.

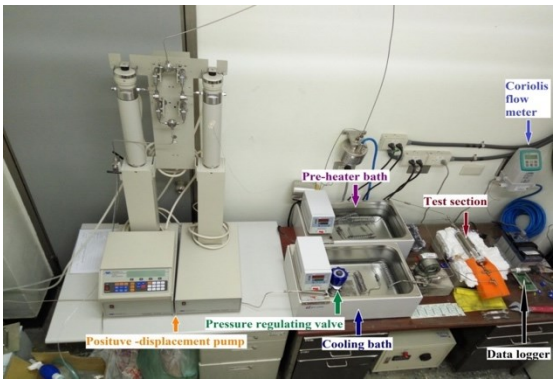


Fig. 5. The photograph of experimental apparatus.

The wall of test section is heated to 200℃. Here, the heated power is about 53W.The Reynolds number is set from 160 to 640(0.33g/s, 0.66g/s and 0.99g/s and 1.32g/s under five kinds of pressure). The analysis shows that the measured uncertainties of temperature, flow rate, pressure, extracted power and heat transfer coefficient are less than ± 0.1℃, $\pm 0.5\%$, $\pm 2.3\%$, $\pm 2.37\%$, and $\pm 10\%$, respectively.

Thermal diffusivity (α) is defined as the ratio of thermal conductivity and specific heat. The thermal dispersion should be considered in the porous media:

$$\alpha_{\text{mean}} = \frac{k_{\text{eff}}}{C_{\text{peff}}} \tag{7}$$

$$k_{eff} = \varepsilon \cdot k_f + (1-\varepsilon) \cdot k_p + \frac{k_{disp,xx}+k_{disp,yy}+k_{disp,zz}}{3} \tag{8}$$

$$C_{peff} = \varepsilon \cdot \rho_f \cdot C_{p,f} + (1-\varepsilon) \cdot \rho_p \cdot C_{p,p} \tag{9}$$

here, k_{eff} is effective thermal conductivity, C_{peff} is specific heat, $k_{disp,xx}$ is the longitude thermal dispersion, $k_{disp,yy}$ is transverse horizontal thermal dispersion, and $k_{disp,zz}$ is transverse vertical thermal dispersion.

$k_{disp,xx}$, $k_{disp,yy}$ and $k_{disp,zz}$ is defined as below:

$$k_{disp,xx} = \frac{(\lambda_{lo}\cdot\overline{ux}^2+\lambda_{trh}\cdot\overline{uy}^2+\lambda_{trv}\cdot\overline{uz}^2)\cdot\rho_f\cdot C_{p,f}}{\sqrt{(\overline{ux}^2+\overline{uy}^2+\overline{uz}^2)_{max}}} \tag{10}$$

$$k_{disp,yy} = \frac{(\lambda_{trh}\cdot\overline{ux}^2+\lambda_{lo}\cdot\overline{uy}^2+\lambda_{trv}\cdot\overline{uz}^2)\cdot\rho_f\cdot C_{p,f}}{\sqrt{(\overline{ux}^2+\overline{uy}^2+\overline{uz}^2)_{max}}} \tag{11}$$

$$k_{disp,zz} = \frac{(\lambda_{trv}\cdot\overline{ux}^2+\lambda_{trv}\cdot\overline{uy}^2+\lambda_{lo}\cdot\overline{uz}^2)\cdot\rho_f\cdot C_{p,f}}{\sqrt{(\overline{ux}^2+\overline{uy}^2+\overline{uz}^2)_{max}}} \tag{12}$$

here, λ_{lo} is longitude thermal dispersivity, λ_{trh} is transverse horizontal thermal dispersivity, λ_{trv} is transverse vertical thermal dispersivity.

The thermal dispersivity of this porous heat transfer model is adjusted from the fitting process of the results of experiment. Through this process, Q (heat extraction) and ΔT (temperature difference between the exit and inlet of test section) of numerical model are close to the results of experiment. From the view of thermal resistance, the model and experiment are similar under the same geometry and thermal-fluid conditions. The model with two kinds of porosity (particle size is 1.54mm and 2.03mm), and 4 inlet mass flow rates (0.00033 kg/s, 0.00066 kg/s and 0.00099 kg/s and 0.00132 kg/s) are processed. Fig. 6 presents the fitting results of this porous heat transfer model. Fig. 6(a) and (b) is the fitting result of the outlet temperature and heat extraction.

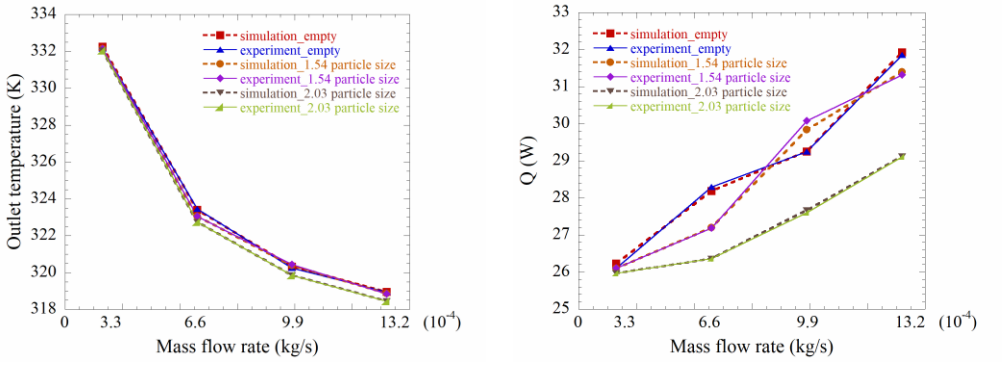


Fig.6 The fitting profiles of outlet temperature and heat extraction with different particle size.

3. OPTIMIZATION

The optimization of heat extraction under the varied pressure and mass flow rate can be obtained as the fitted simulated model is built. The numerical design approach is developed by combining a direct problem solver, COMSOL code, with an optimal method (the simplified conjugate gradient method, SCGM). The COMSOLpackage is used as the subroutine to solve the temperature profiles associated with the variation of the pressure, mass flow rate of the single well during the iterative optimal process. The SCGM method is capable of obtaining the minimized objective functions easily, and calculating fast than traditional conjugated gradient method. In the SCGM method, the sensitivity of the objective function resulted from the designed variables is evaluated first, and then by giving an appropriate fixed value for the step size, the optimal design can then be carried out without overwhelming mathematical derivation.

The heat extraction through the reservoir is chosen be the objective function, J , of this study, and the maximum objective function will be approached through the optimization.

$$\mathrm{J} = \mathrm{Q} \tag{13}$$

Assume that, a set of undetermined coefficients will be optimized in the iterative process. Different combinations of these coefficients represent the variation of the operation of heat extraction. The optimal values of these coefficients were determined using an iterative scheme based on the SCGM optimization method and COMSOL finite element analysis software. The iterative scheme and optimization criteria are illustrated as below.

Let $\{a_i, i = 1,2,...,k\}$ be the set of the undetermined coefficients. In other words, in the optimization process, the coefficients $\{a_i, i = 1,2,...,k\}$ are updated iteratively toward the minimization of the object function.The method evaluates the gradient functions of the objective function and sets up a new conjugate direction for the updated undetermined coefficients with the help of a direct numerical sensitivity analysis.

We perform the direct numerical sensitivity analysis to determine the gradient functions $(\partial J/\partial a_i)^n, (i = 1,2,...,l)$. First, give a perturbation (Δa_i) to each of the undetermined coefficients, $\{a_i, i = 1,2,...,l\}$, and then find the change in the objective function (ΔJ) caused by Δa_i. The gradient function with respect to each of the undetermined coefficients $\{a_i, i = 1,2,...,l\}$ can be calculated by the direct numerical differentiation as

$$\frac{\partial J}{\partial a_i} = \frac{\Delta J}{\Delta a_i} \tag{14}$$

Then, we can calculate the conjugate gradient coefficients, γ_i^n , and the search directions, π_i^{n+1} , for each of the undetermined coefficients $\{a_i, i = 1,2,...,l\}$ with

$$\gamma_i^n = \left[\frac{\left(\frac{\partial J}{\partial a_i}\right)^n}{\left(\frac{\partial J}{\partial a_i}\right)^{n-1}} \right]^2, \quad i = 1,2,...,l \tag{15}$$

$$\pi_i^{n+1} = \left(\frac{\partial J}{\partial a_i}\right)^n + \gamma_i^n \pi_i^n, \quad i = 1,2,...,l \tag{16}$$

The step sizes $\{\beta_i, i=1,2,...,I\}$ will be assigned for all the undetermined coefficients $\{a_i, i=1,2,...,I\}$ and leave it unchanged during the iteration.

$$a_i^{n+1} = a_i^n - \beta_i \pi_i^{n+1}, \quad i=1,2,...,I \tag{17}$$

Meanwhile, the COMSOL package is used to solve the temperature profile associated with each set of undetermined coefficients considered in the iterative SCGM procedure. The step size of the iterative process is determined by a trial and error process, and the value is set as 1×10^{-4} for this case.

It mentions that the emphasis of the present study is put on the optimization of the heat extraction. To the authors' knowledge, it's a new view to deal the heat extraction problem of gerthermics from the point of the porous heat transfer by using the combination of numerical package and self-developed optimal method. The flow chart of the optimal process is shown in Fig. 7 and described briefly as follows:

(1) Make an initial guess regarding the shape profile by giving initial values to the set of undetermined coefficients. With initialization accomplished, the run itself can begin.

(2) Use the direct problem solver to predict the temperature profile of the reservoir, and calculate the objective function J using Eq. (13).

(3) When the objective function reaches a minimum, that is to say, the relative criteria is satisfied, the solution process is terminated; otherwise, proceed to Step (4).

(4) Use Eq. (14) to determine the gradient functions.

(5) Use Eqs. (15) and (16) to calculate the conjugate gradient coefficients, γ_i^n, and the search directions, π_i^{n+1}, for each of the undetermined coefficients.

(6) Assign a fixed value to the step sizes for all the undetermined coefficients and leave it unchanged during the iteration.

(7) Employ Eq. (17), to update the undetermined coefficients and renew the operated conditions of the heat extraction, and then go back to Step (2).

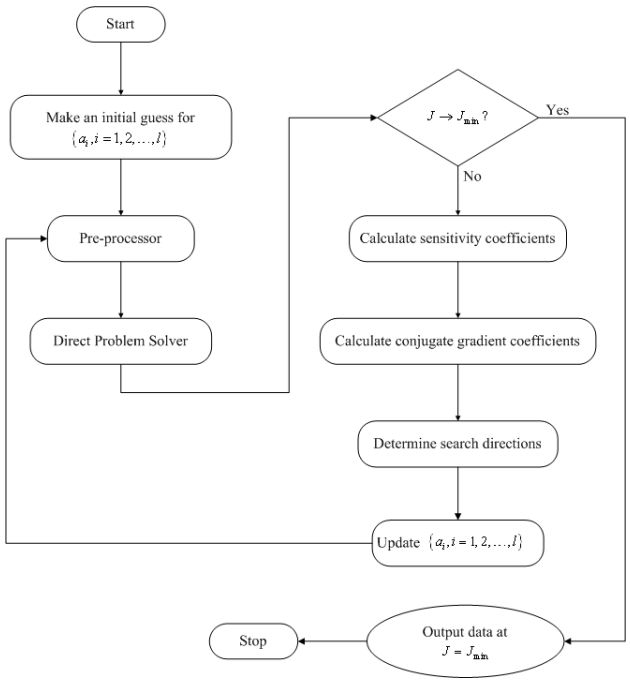


Fig. 7 The flow chart of the optimal process

Based on the fitted simulated model and the capacity test of IC13, Chingshui, Taiwan, four kinds of capacity test are discussed to process the optimization.

The location of IC13, Chingshui, Taiwan is shown in Fig. 8 and the results of capacity test are listed in Table 1.

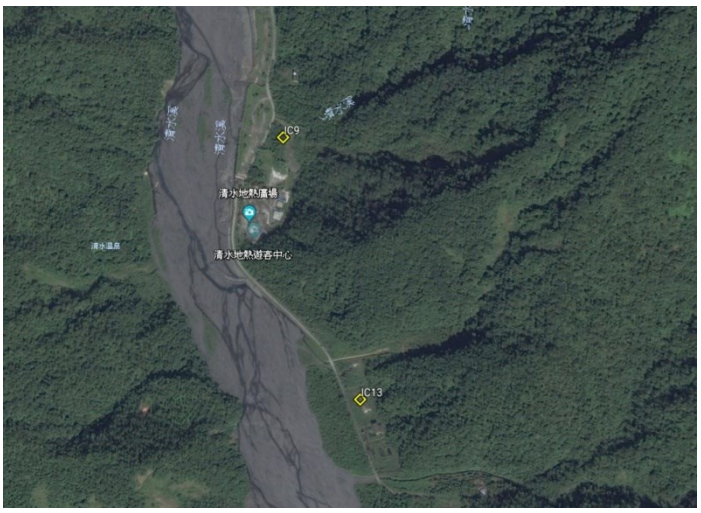


Fig. 8 The location of IC13, Chingshui, Taiwan

Table 1 The capacity test of IC13, Chingshui, Taiwan

Depth (M)	Pipe diameter(in)	Bottom temperature(° C)	Wellhead pressure (Kg/cm2)	total flow rate (ton/hr)	Steam (ton/hr)	Heat water (ton/hr)	Wellhead temperature(° C)	Date
1275.02	35mm	>217.1	12.5	25.5	6.8	18.7	180	2017/10/26
1275.02	1.5	>217.1	14.2	31.2	5.2	26	185	2009/7/8-9
1275.02	2	>217.1	9.3	34.7	8.7	26	173.7	2009/7/9-10
1275.02	2.5	>217.1	7.3	39.7	12.3	27.4	164.3	2009/7/10-11

The depth of well of IC13 is 1275.02 m and the temperature of well bottom is 217.1 °C. The test tube of capacity test is 35 mm, 1.5 in, 2 in and 2.5 in, separately. The flow rate of steam, water and temperature of wellhead are listed in Table 1. Fig. 8 shows the temperature profiles of well with the different test tube. Then, the thermal resistance can be obtained from the temperature difference between the well and environment. The heat extraction and thermal resistance with the different test tube is shown in Fig. 9. Throughout the Fig. 9 (a), the heat extraction increases linearly as the test tube increases. In addition, the heat extraction of the capacity test of 35 mm in 2017 and 1.5 inches in 2009 is 0.97 MW and 1.04 MW. It can prove that this well keep on a stable condition for a long time. The thermal resistance is about 550 K/MW-Kg from the average of the results Fig. 9 (b). Through the optimization, the iteration of temperature of wellhead and the velocity is shown in Fig. 10. Finally, the temperature of wellhead keeps on 458.17K even the velocity still increases through the optimization.

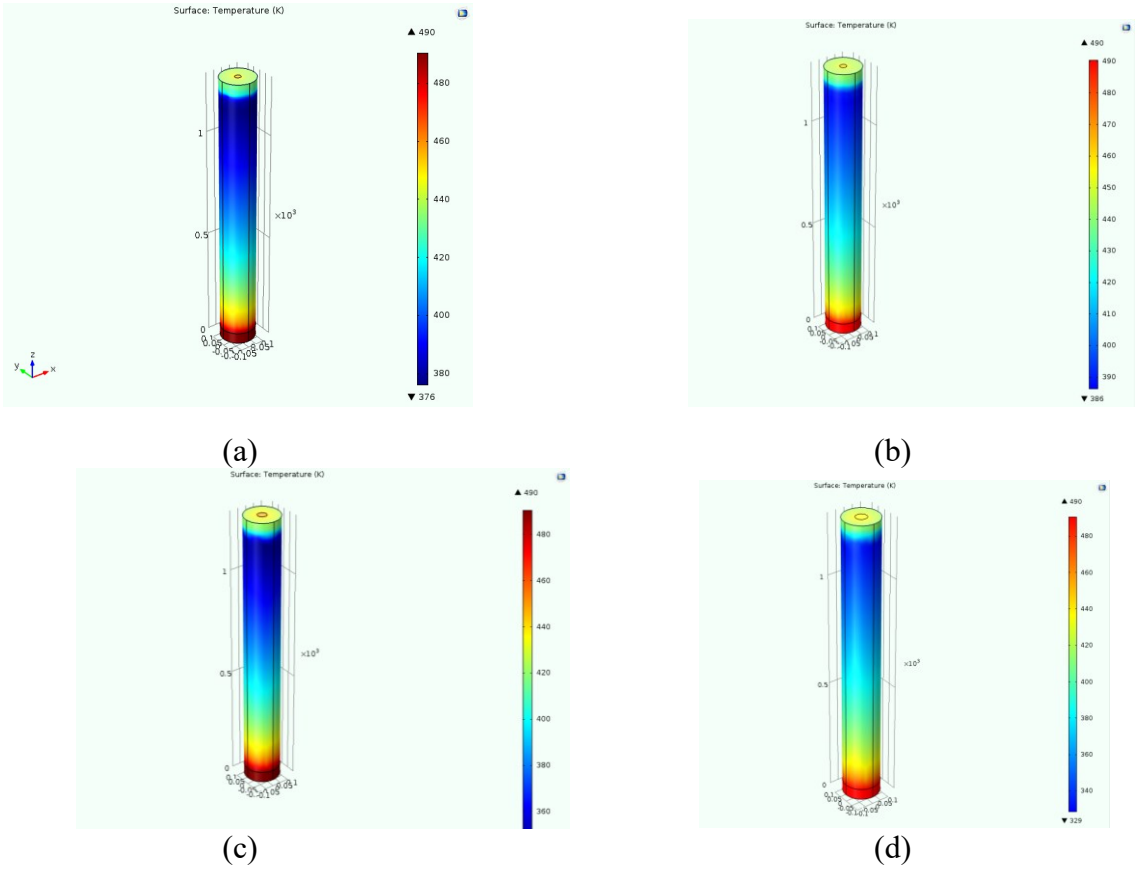


Fig. 8 The temperature profile of IC13 (a)35 mm,(b)1.5 in,(c)2 in,(d) 2.5 in

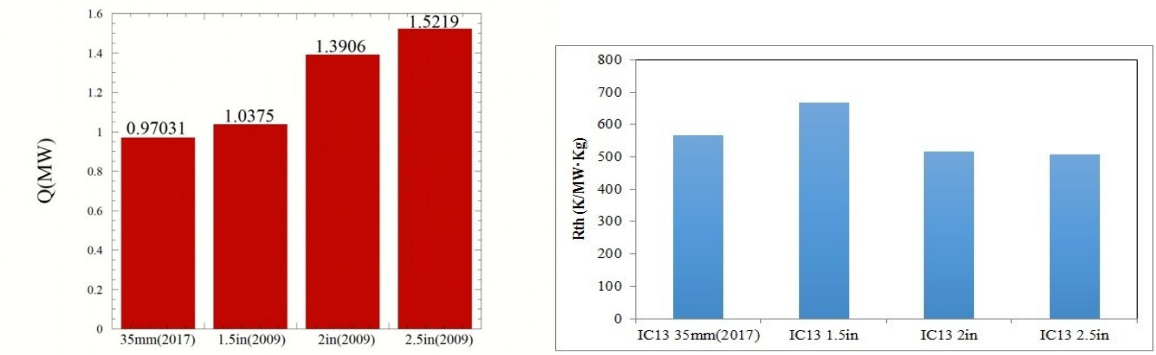


Fig. 9 The (a) heat extraction and (b) thermal resistance with difference test tube

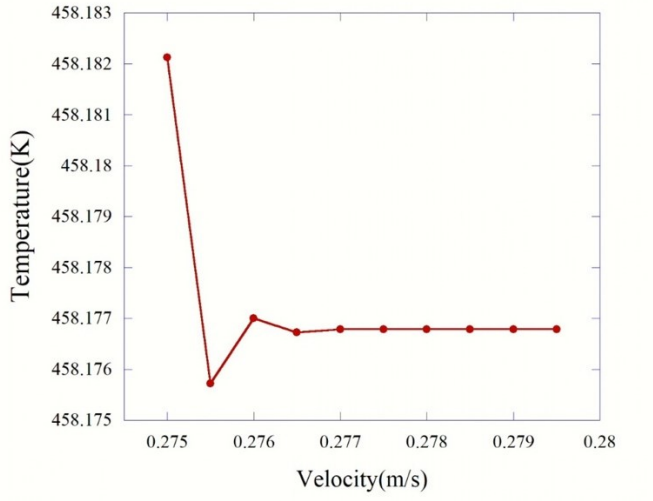


Fig. 10 The optimization of temperature and velocity in 1.5 in test tube

4. CONCLUSION

An innovative similar capacity test model is proposed. In this model, the porous TH model and in-situ information is conjugated to obtain the thermal resistance of single well. Therefore, the optimization can be processed for obtaining the optimal mass flow rate based on the best heat extraction. In this study, a model of IC 13 in Chingshui, Taiwan is bulit. This model improves that the thermal resistance can be one of the characteristics of single well. The best heat extraction is obtained based on the fixed thermal resistance.

REFERENCES

Biagi, J., Agarwal, R., and Zhang, Z.: Simulation and optimization of enhanced geothermal systems using CO_2 as a working fluid, *Energy*, **86**, (2015), 627-637.

Cao, W., Huang, W., and Jiang, F.: A novel thermal–hydraulic–mechanical model for the enhanced geothermal system heat extraction, *Int. J. Heat and Mass Transfer*, **100**, (2016), 661-671.

Chen, J. and Jiang, F.: Designing multi-well layout for enhanced geothermal system to better exploit hot dry rock geothermal energy, *Renewable Energy*, **74**, (2015), 37-48.

Cladouhos, T.T., Petty, S., Swyer, M.W., Uddenberg, M.E., Grasso, K., and Nordin, Y.: Results from Newberry Volcano EGS Demonstration, 2010–2014, *Geothermics*, **63**, (2016), 44-61.

Gallup, D.L.: Production engineering in geothermal technology: a review, *Geothermics*, **38**, (2009), 326-334.

Jacquey, A.B., Cacace, M., Blöcher, G., Watanabe, N., Huenges, E., and Scheck-Wenderoth, M.: Thermo-poroelastic numerical modelling for enhanced geothermal system performance: Case study of the Groß Schönebeck reservoir, *Tectonophysics*, **684**, (2016), 119-130.

Jeanne, P., Rutqvist, J., Hartline, C., Garcia, J., Dobson, P.F., and Walters, M.: Reservoir structure and properties from geomechanical modeling and microseismicity analyses associated with an enhanced geothermal system at The Geysers, California, *Geothermics*, **51**, (2014), 460-469.

Jiang, F., Chen, J., Huang, W., and Luo, L.: A three-dimensional transient model for EGS subsurface thermo-hydraulic process, *Energy* **72**, (2014), 300-310.

Kim, S., and Hosseini, S. A.: Hydro-thermo-mechanical analysis during injection of cold fluid into a geologic formation, *Int. J. of Rock Mechanics and Mining Sciences*, **77**, (2015), 220-236.

Lin, D.T.W., Hsieh, J.C., Shih, P.Y.: Optimization of operating condition of geothermal system based on supercritical CO_2 heat extraction, *Renewable Energy*, **143**, (2019), 1162-1171.

Llanos, E.M., Zarrouk, S.J., and Hogarth, R.A.: Numerical model of the Habanero geothermal reservoir, Australia, *Geothermics* **53**, (2015), 308-319.

Shook, G.M., and Suzuki, A.: Use of tracers and temperature to estimate fracture surface area for EGS reservoirs, *Geothermics*, **67**, (2017), 40-47.

Sun, Z.X., Zhang, X., Xu, Y., Yao, J., Wang, H.X., Lv, S., Sun, Z.L., Huang, Y., Cai, M.Y., and Huang, X.: Numerical simulation of the heat extraction in EGS with thermal-hydraulic-mechanical coupling method based on discrete fractures model, *Energy*, **120**, (2017), 20-33.

Verma, A., and Pruess, K.: Enhancement of Steam Phase Relative Permeability Due to Phase Transformation Effects in Porous Media, *Proceedings,* 11th Workshop on Geothermal Reservoir Engineering, Stanford University, Stanford, CA (1986).